

The formation of Kuiper-belt Binaries through Exchange Reactions

Yoko Funato^{1*}, Junichiro Makino², Piet Hut³,
Eiichiro Kokubo⁴ & Daisuke Kinoshita⁵

¹ General System Studies, University of Tokyo, Komaba, Meguro-ku, Tokyo 153, Japan

² Department of Astronomy, University of Tokyo, Hongo, Bunkyo-ku, Tokyo 113, Japan,

³ Institute for Advanced Study, Princeton, NJ 08540, USA

⁴ National Astronomical Observatory, Osawa, Mitaka-shi, Tokyo 180, Japan

⁵ National Central University, Chung-Li 32054 Taiwan

Recent observations ^{1–6} have revealed an unexpectedly high binary fraction among the Trans-Neptunian Objects (TNOs) that populate the Kuiper-belt. The discovered binaries have four characteristics they comprise a few percent of the TNOs, the mass ratio of their components is close to unity, their internal orbits are highly eccentric, and the orbits are more than 100 times wider than the primary's radius. In contrast, theories of binary asteroid formation tend to produce close, circular binaries. Therefore, a new approach is required to explain the unique characteristics of the TNO binaries. Two models have been proposed^{7, 8}. Both, however, require extreme assumptions on the size distribution of TNOs. Here we show a mechanism which is guaranteed to produce binaries of the required type during the early TNO growth phase, based on only one plausible assumption, namely that initially TNOs were formed through gravitational instabilities⁹ of the protoplanetary dust layer.

The TNO binary with best known orbital elements, 1998WW31, has a mass ratio $m_2/m_1 \sim 0.7$, eccentricity $e \sim 0.8$, and semi-major axis $a \sim 2 \times 10^4$ km. The inferred radii of the components are $r_1 \sim 1.1r_2 \sim 10^2$ km, hence $a/r_1 > 10^2$, in stark contrast to main belt asteroid binaries where $m_2/m_1 \ll 1$, $e \sim 0$, and $a/r_1 \lesssim 10$. Asteroid binaries in the main belt are probably formed by collisions¹⁰, as in the leading theory for the formation

*funato@chianti.c.u-tokyo.ac.jp

of the Moon^{11, 12}, which naturally explains the extreme mass ratios and tight near-circular orbits^{13, 14}.

In order to find a completely different process for TNO binaries, we can borrow ideas from dynamical binary formation in star clusters, where many roughly equal-mass binaries are found. There, we know of three formation paths: 1) two-body dissipational encounters¹⁵; 2) three-body binary formation¹⁶; and 3) exchange reactions¹⁶. Figure 1 schematically shows these paths.

In the case of TNOs and asteroids, path 1 corresponds to the standard theory for binary formation, namely tidal disruption and giant impact during a close encounter (**a** and **b** in Figure 1). They indeed occur: each TNO has grown through accretion, and much of accretion has happened through collisions with an object comparable in mass to that of the growing TNO itself^{17, 18}.

Path 2 (**c** in Figure 1) would require a near-simultaneous encounter of three massive objects with low enough velocities to allow an appreciable chance to leave two of the objects bound. For this to work, the random velocities of the most massive objects should be significantly lower than their Hill velocities, $v_H \equiv R_H \Omega(R)$, where R_H is the Hill radius of the asteroid at a distance R from the Sun and $\Omega(R)$ is its orbital angular velocity. This path could work if there are $\sim 10^5$ 100 km-sized objects embedded in a sea of small (< 1 km) objects⁸. This assumption, however, is at odds with Goldreich and Ward's theory for the formation of planetesimals⁹ through gravitational instability, and it is hard to see how objects in the Kuiper-belt could form from non-gravitational coagulation, because the time scales are far too long¹⁹. In contrast, the gravitational instability theory predicts the size of the initial bodies to be 10 – 100km. Starting with these bodies would make path 2 ineffective, because the velocity dispersion would be higher than the Hill velocity^{17, 20}.

A combination of paths 1 and 2 has been proposed⁷. It was studied how a third massive body could capture a collision product of two massive bodies if the third body were near enough during the time of the collision. This mechanism seems unlikely to work, since it requires a number density of massive objects about two orders of magnitude higher than the value consistent with observations⁸.

Another mechanism based on the dynamical friction from smaller bodies that can let a hyperbolic encounter between two massive bodies produce a bound orbit has been proposed⁸. As we mentioned above, the gravitational instability theory for the formation of planetesimals⁹ would exclude the existence of such a sea of small objects.

Path 3 (**d** in Figure 1) can operate on the binaries formed through path 1 (**b** in Figure 1), so we should check whether paths 1 and 3 together produce the right binaries in the right numbers.

Consider a relatively massive TNO primary with mass m_1 , in a binary with a secondary with mass $m_2 \ll m_1$. If the binary encounters another body with mass $m_3 \sim m_1$, the

most likely result is an exchange reaction, in which the incoming object replaces the original secondary²¹. Figure 2 shows an example of such a reaction.

If the incoming velocity of the third body is small, the binding energy of the resulting binary is comparable to or larger than that of the initial binary, since otherwise the secondary could not escape. In practice, the change in binding energy is relatively small, as will be shown later. Hence $m_1 m_2 / a_0 \approx m_1^2 / a$ where a is the new semi-major axis after the exchange. This implies $a/a_0 \approx m_1/m_2 \gg 1$.

For the exchange reaction to occur, the third body should approach the binary to a distance comparable to a_0 . The angular momentum carried away by the light body is small. Therefore, the periastron distance of the resulted binary is comparable to that of the initial parabolic orbit, in other words, to a_0 . Thus, the eccentricity is $e \sim 1 - a_0/a \sim 1 - m_2/m_1$.

We have run a series of numerical scattering experiments to obtain cross sections for different outcomes of binary-single body interactions (see Methods for details). The results show that 80% of the cross sections corresponding to the change of the composition of the binary is accounted for by processes leading to the formation of binaries with two massive components. In figure 3 the distribution for the semi-major axis is strongly peaked around $a \sim 20$. This result is in good agreement with the simple argument presented above. This peak arises from the exchanges which take place at the first binary-single body encounter. The broad peak around $a \sim 10$ arises from “resonant encounters”, in which encounters of two objects occur more than two times²³. The eccentricity peaks at 0.95, as expected. In the case of 1998WW31 with $r_1 = 75\text{km}$, our length unit corresponds to 1500 km. In figures 2 and 3 we attach this physical scale to give a concrete idea of the size. Figure 4 clearly shows that the orbital elements of 1998WW31 are consistent with the binary having formed through the processes modeled here.

We now confront our second task: to check whether the exchange path is efficient enough to produce the observed binaries. Starting with TNOs formed through gravitational instability of the protoplanetary dust layer⁹, the heaviest TNOs will accrete mass primarily through collisions with TNOs of comparable mass^{17, 18}. Many of these collisions are of the “giant impact” type, resulting in tight strongly unequal-mass binaries (**b** in Figure 1). Let us estimate how many such binaries are formed and what fraction of them are converted to wide binaries through exchange.

We assume that one in three collisions between comparable TNOs gives rise to a binary¹⁴. The numerical simulations of planetesimal collisions yield a sizable formation rate of satellites of 43.3 %¹⁴. Since the relative velocity between objects in the TNO region is significantly lower than that assumed in their simulations, the corresponding binary formation rate in the TNO region is even higher. To stay on the conservative side, however, we have assumed a ratio of only 1/3.

In 2/3 of the cases when no binary is produced, we have to wait for a typical time T

until another collision occurs. When a binary is formed, the cross section for subsequent interactions with a third body, taking into account gravitational focusing, is in proportion to a_0 . Therefore, our newly-formed binary will undergo an exchange reaction on a time scale $(r/a_0)T \ll T$, leading to a significant increase in a . Strong three-body interactions will subsequently occur on an shorter time scale $(r/a)T \ll T$. As a result, the semi-major axis will shrink systematically, with a ‘thermal’ distribution $f(e) = 2e$ favoring high eccentricity¹⁶. When the orbit becomes small enough ($r/a \sim 0.03$), the change for collisions in resonant encounters becomes significant²⁴.

Let us assume that an exchange reaction turns a “giant impact” binary into a binary with $a \sim 300r$. Each subsequent strong encounter will on average shrink a by a factor²⁵ ~ 1.2 . After a dozen encounters, $a \sim 30r$ and a collision is likely to occur. The time scale for each encounter to occur is $\sim (r/a)T$, and the waiting time for the last encounter in this series is $(1/30)T$. Summing this series, we get a total waiting time of $(T/30)/(1 - (1/1.2)) = 0.2T$ before a collision. If three bodies collide, or if the third body escapes, the resulting system may be a single body (with an assumed chance of 2/3) or a strongly unequal-mass binary (a chance of 1/3). If the merger product and the third body are still bound, we have an equal-mass wide binary.

Under these assumptions, in 1/3 of the cases, we wind up with an equal-mass TNO binary with the observed properties for a period $\sim 0.2T$, compared to a 2/3 chance to wind up with a single TNO for a period $\sim T$. Denoting by N_S and N_B the number of single bodies and the number of binaries, respectively, we have

$$\begin{aligned}\frac{dN_B}{dt} &= \frac{1}{3}N_S - \frac{1}{0.2} \frac{2}{3}N_B \\ \frac{dN_S}{dt} &= -\frac{dN_B}{dt}\end{aligned}$$

if we measure time in units of T . For the stationary state we have $dN_B/dt = dN_S/dt = 0$, and $N_B = 0.1N_S$. Therefore, the predicted binary fraction is $\sim 10\%$. When accretion in the Kuiper-belt region diminished, the number of single and binary objects was frozen, with a ratio similar to this steady-state value.

While our arguments are approximate, it is clear that after cessation of the accretion stage at least several percent of the TNOs were accidentally left in such a binary phase. The fact that more than 1% of the known TNOs are found to be in wide roughly equal-mass binaries is thus a natural consequence of *any* accretion model *independent of the assumed parameters* for the density and velocity dispersion of the protoplanetary disk or the duration of the accretion phase. We predict that future discoveries of TNO binaries will similarly show roughly equal masses, large separations, and high eccentricities.

Methods

Numerical scattering experiments We performed 775,541 runs of numerical integrations of binary-single body encounters. We chose the relative velocity v_∞ between the intruder (single body) and the binary at infinity to be much smaller than the orbital velocity of the binary components. In this regime, the scattering cross section σ is expressed as $\sigma \propto \sigma_0/v_\infty^2$, because of gravitational focusing^{7, 25}. The parabolic orbit is the limiting case of $v_\infty \rightarrow 0$ where the nominal cross section σ diverges, but σ_0 converges to a finite value.

We fixed the initial orbital parameters of the binary, and changed the relative orbit of the intruder to obtain scattering cross sections. For encounters with finite v_∞ , one should randomly change the direction of v_∞ and also randomly select impact parameter vectors uniformly within a circle of given radius. This radius should be large enough so that encounters with impact parameter larger than this radius would not result in exchange or collision. For parabolic encounters, this procedure choice corresponds to choosing the periastron distance r_p from a uniform distribution with an upper limit and selecting random orientations for the orbital plane and direction of the periastron. As an upper limit, we chose $20a_0$, where a_0 is the semi-major axis of the initial binary. Initial separations between the intruder and the binary were $100a_0$.

We use units in which $G = m_1 = m_3 = a_0 = 1$, where G is the gravitational constant, m_1 and m_3 are the masses of the heavier body of the initial binary and the intruder. The mass of the secondary component is $m_2 = 0.05$. The radii of the bodies are $r_1 = r_3 = 0.05$ and $r_2 = r_1(m_2/m_1)^{1/3} \approx 0.01842$. The initial binary is circular. These values are typical for main-belt binary asteroids, with $m_2/m_1 < 0.1$, and separations are 5 – 40 times the radius of the primary.

We terminated the numerical integration when (a) one of the three bodies escaped beyond the Hill radius, or (b) when two bodies physically collided. For (a) we chose a Hill radius of $r_H = 100a_0$, since a typical value for a TNO with radius r , $m = 10^{21}$ g and $R = 40$ AU is $a = 1000r$, and the typical semi-major axis of a close, circular planetesimal binary is $a_0 = 10r$. When a collision occurred, the collision product was assumed to inherit the mass and motion of the center of mass of the two bodies. We adapted the radius so as to conserve the density. In both cases, we calculated the orbit of the remaining two bodies to determine the final state.

We integrated the equations of motion of the three bodies in Cartesian coordinates. Integration was done with an 8th order time-symmetric variable-stepsizes Hermite method. To cross-check the results, we also performed two other sets of scattering experiments, one using the scattering package of STARLAB²², and the other using a 4th order Hermite scheme. In all cases, we used completely different programs for generating initial conditions, as well as for orbit integration and for the reduction of the results. All three experiments gave the

same outcome, within the expected fluctuations associated with the finite number of runs. There are six possible configuration changes that can take place as a result of a scattering event: (a) an exchange reaction resulting in a massive–massive binary; (b) an exchange reaction resulting in a massive–light binary; (c) a merger of bodies 1 and 2 resulting in a massive–massive binary; (d) a merger resulting in a twice-as-massive–light binary; (e) a merger of bodies 2 and 3 resulting in a massive–massive binary; (f) no binary is left, after three-body merging or two-body merging followed by escape.

The cross section σ_0 for each event is as follows: (a) 12.1 (b) 1.3 (c) 0.9 (d) 1.3 (e) 0.9 (f) 1.2 in our units. For our scattering experiments with $r_p < 20a_0$, we found a cross section for preservation of the original binary of 1243.9 in our units, which implies that in 99 % of our experiments no configuration change took place. We also found that for $r_p > 20a_0$ no merger or exchange occurred, so our cross section measurements are complete.

Another logical possibility would be: (g) all three objects become unbound. However, for that to occur the total energy would have to be positive. In our case, the low relative velocity of the incoming third body guarantees the total energy to be negative, hence (g) cannot occur.

The physical reason for the dominance of (a) is the statistical tendency for equipartition of kinetic energy, which implies much higher velocities for much lighter bodies and therefore a much larger chance for those lighter bodies to escape.

We acknowledge helpful comments on our manuscript by Peter Goldreich, Roman Rafikov, Re'em Sari, Keith S. Noll and Dan Durda.

1. Burns, J. A., “Two Bodies Are Better Than One”, *Science*, 297, 942-943 (2002).
2. Veillet C., et al., “The binary Kuiper-belt object 1998 WW 31”, *Nature*, 416, 711-713 (2002).
3. Margot, J-L., “Worlds of mutual motion”, *Nature*, 416, 694-695, (2002).
4. Noll, K. S. ,Stephens, D. C. , Grundy, W. M. , Millis, R. L. , Spencer, J. , Buie, M. W. , Tegler, S. C. , Romanishin, W. and Cruikshank, D. P., “Detection of Two Binary Trans-Neptunian Objects, 1997 CQ₂₉ and 2000 CF₁₀₅, with the Hubble Space Telescope” , *Astronomical Journal*, 124, 3424-3429. (2002).
5. E.L. Schaller, E. L., and Brown M. E., “A Deep Keck Search for Binary Kuiper Belt Objects”, DPS 35th Meeting, abstract no. 39.20 (2003).
6. Noll, K. S., Stephens, D., Grundy, W., Tegler, S., Romanishin, W., Cruikshank, D., “Discovery of transneptunian binaries with HST”, DPS 35th Meeting, abstract no. 49.07 (2003).

7. Weidenschilling, S. J., "On the Origin of Binary Transneptunian Objects", *Icarus*, 160, 212-215 (2002).
8. Goldreich, P., Lithwick, Y., and Sari, R., "Formation of Kuiper-belt binaries by dynamical friction and three-body encounters", *Nature*, 420, 643-646 (2002).
9. Goldreich, P. and Ward, W. R., "The Formation of Planetesimals", *Astrophysical Journal*, 183, 1051-1062 (1973).
10. Merline, W. J., Weidenschilling, S. J., Durda, D. D., Margot, J. L., Pravec, P., and Storrs, A. D., "Asteroids Do Have Satellites", in *Asteroids III* eds Bottke, W. F., Cellino, A., Paolicchi, P. & Binzel, R. P. 273-287 (2003).
11. Hartmann, W. K. and Davis, D. R., "Satellite-sized planetesimals and lunar origin", *Icarus*, 24, 504-515 (1975).
12. Kokubo, E., Ida, S., Makino, J. "Evolution of a Circumterrestrial Disk and Formation of a Single Moon", *Icarus*, 148, 419-436, (2000).
13. Durda, D. D., Bottke, W. F., Asphaug, E., and Richardson, D. C., "The Formation of Asteroid Satellites: Numerical Simulations Using SPH and N-body Models", *Bull. Am. Astron. Soc.*, 33, 1134 (2001).
14. Durda, D. D., W. F. Bottke, B. L. Enke, E. Asphaug, D. C. Richardson, and Z. M. Leinhardt "The formation of asteroid satellites in catastrophic impacts: Results from numerical simulations" *Lunar Plan. Sci. XXXIV*, abstract no. 1943. (2003).
15. Fabian, A.C., Pringle, J.E. & Rees, M.J., "Tidal capture formation of binary systems and X-ray sources in globular clusters", *Monthly Notices of Royal Astronomical Society*, 172, 15-18 (1975).
16. Heggie, D.C., "Binary evolution in stellar dynamics", *Monthly Notices of Royal Astronomical Society*, 173, 729-787 (1975).
17. Kokubo, E. and Ida, S., "Oligarchic Growth of Protoplanets", *Icarus*, 131, 171-178 (1998).
18. Makino, J., Fukushige, T., Funato, Y., & Kokubo, E., "On the mass distribution of planetesimals in the early runaway stage", *New Astronomy*, 3, 411-416 (1998)
19. Wetherill, G.W., "Formation of the earth", *Annu. Rev. Earth Planet. Sci.* 18, 205-256 (1990).
20. Kenyon, S. J. and Luu, J. X., "Accretion in the Early Kuiper Belt. I. Coagulation and Velocity Evolution", *Astronomical Journal*, 115, 2125-2160 (1998).

21. Spitzer, L., *Dynamical evolution of globular clusters*, Princeton, NJ, Princeton Univ. Pr., (1987).
22. McMillan, S. & Hut, P., "Binary-Single-Star Scattering. VI. Automatic Determination of Interaction Cross Sections", *Astrophysical Journal*, 467, 348-358 (1996).
23. Hut, P., "Hard Binary-Single Star Scattering Cross Sections For Equal Masses" *Astrophysical Journal Supplement*, 55, 301-317 (1984).
24. Hut, P. and Inagaki, S., "Globular cluster evolution with finite-size stars - Cross sections and reaction rates", *Astrophysical Journal*, 298, 502-520 (1985).
25. Heggie, D.C. & Hut, P. *The Gravitational Million-Body Problem*, Cambridge, London, Cambridge Univ. Pr., Ch. 23 (2003).

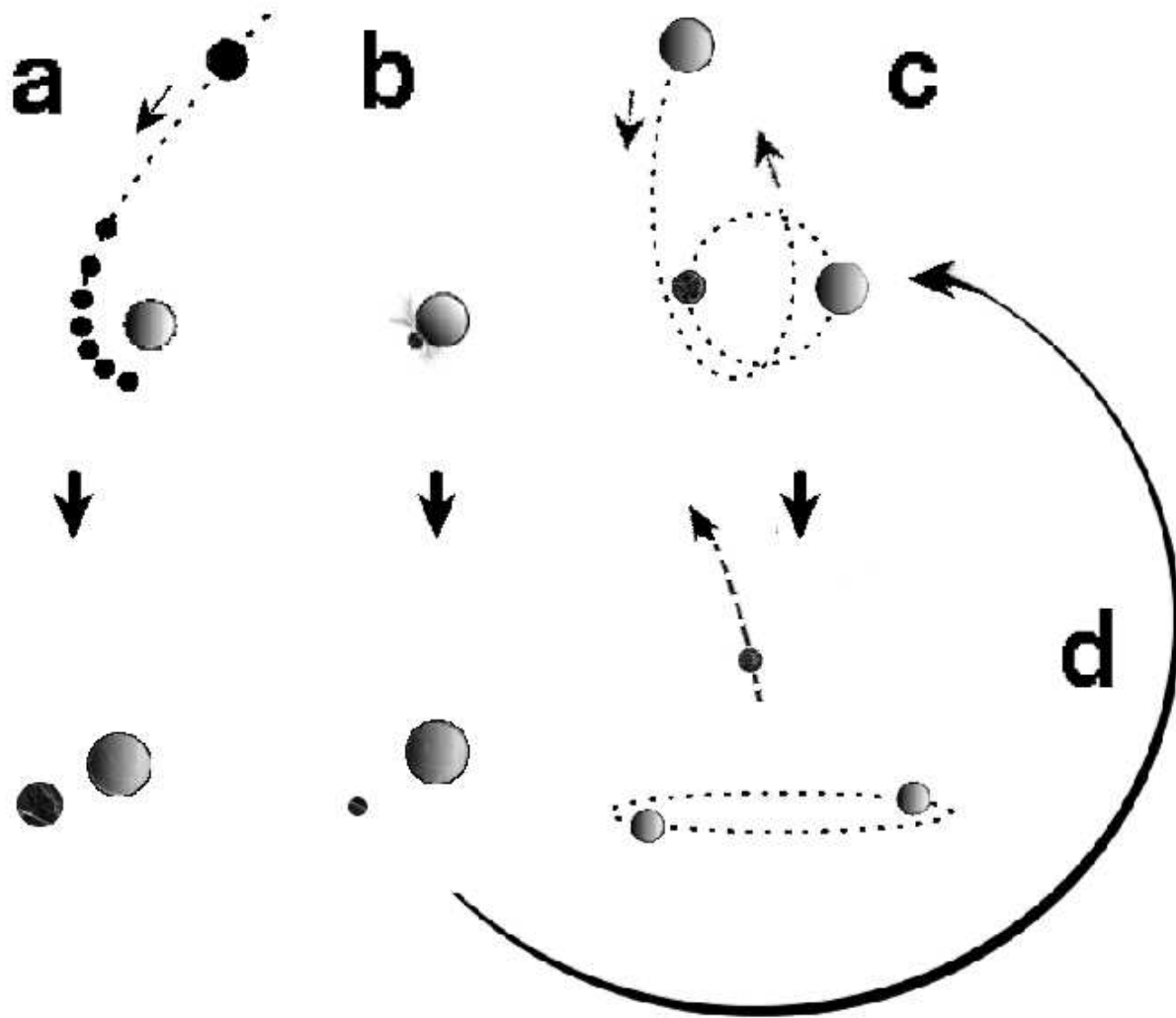


Figure 1: Paths of formation of binaries. Path (a) is the formation through tidal disruption of one object followed by coagulation of fragments during a close encounter with the other; (b) a giant impact, where collision debris coagulates into a “moon”; (c) an exchange reaction, where the incoming body replaces one component of a binary; (d) a combination of (b) and (c).

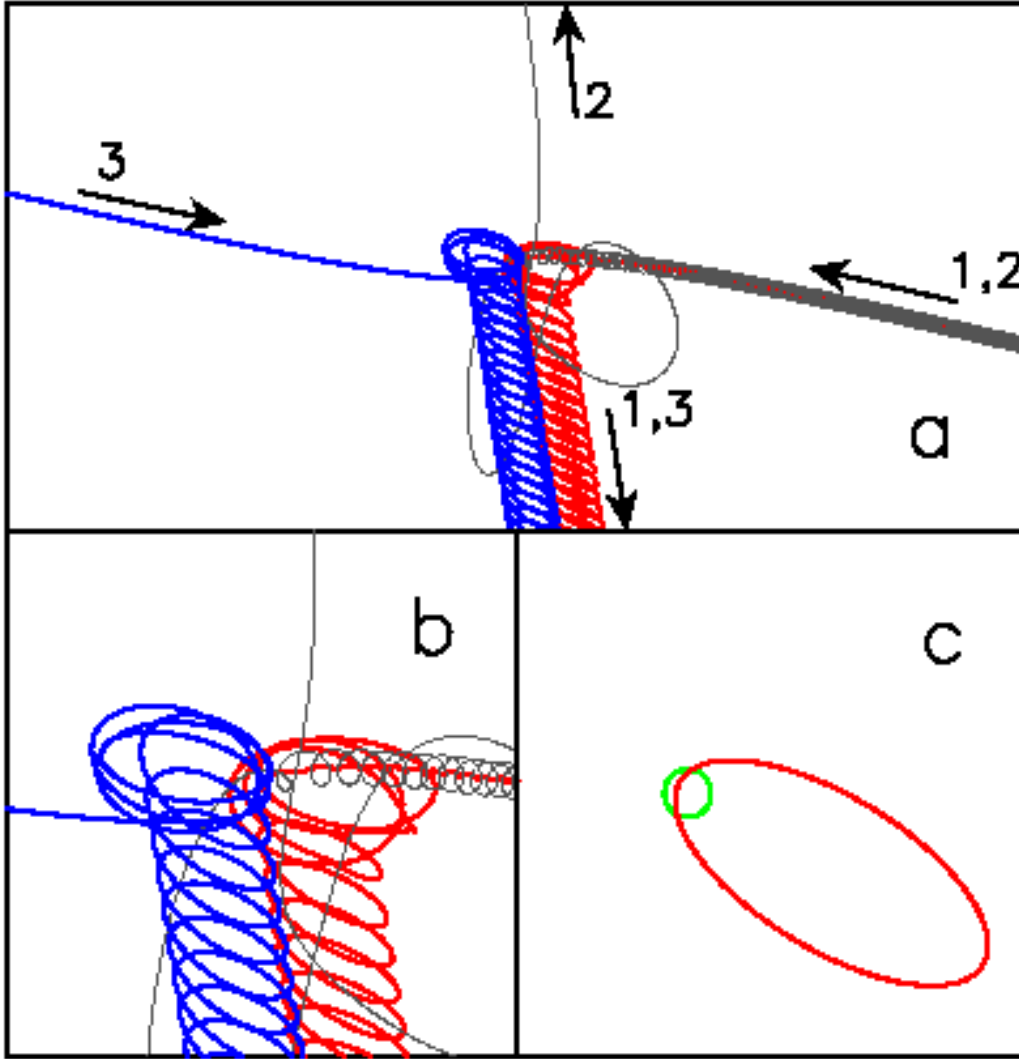


Figure 2: An example of a binary–single-body exchange interaction. Bodies 1 and 2 having masses $m_1 = 1$ and $m_2 = 0.1$, respectively, form a binary with an initially circular orbit. Body 3, with mass $m_3 = 1$, encounters the binary on an initially parabolic orbit. In panel **a**, the whole scattering process is shown. Panel **b** shows the complex central interaction in more detail, while panel **c** shows the orbits of the initial (green) and final (red) binary, respectively. The final binary orbit is highly eccentric and much wider than the initial circular binary orbit.

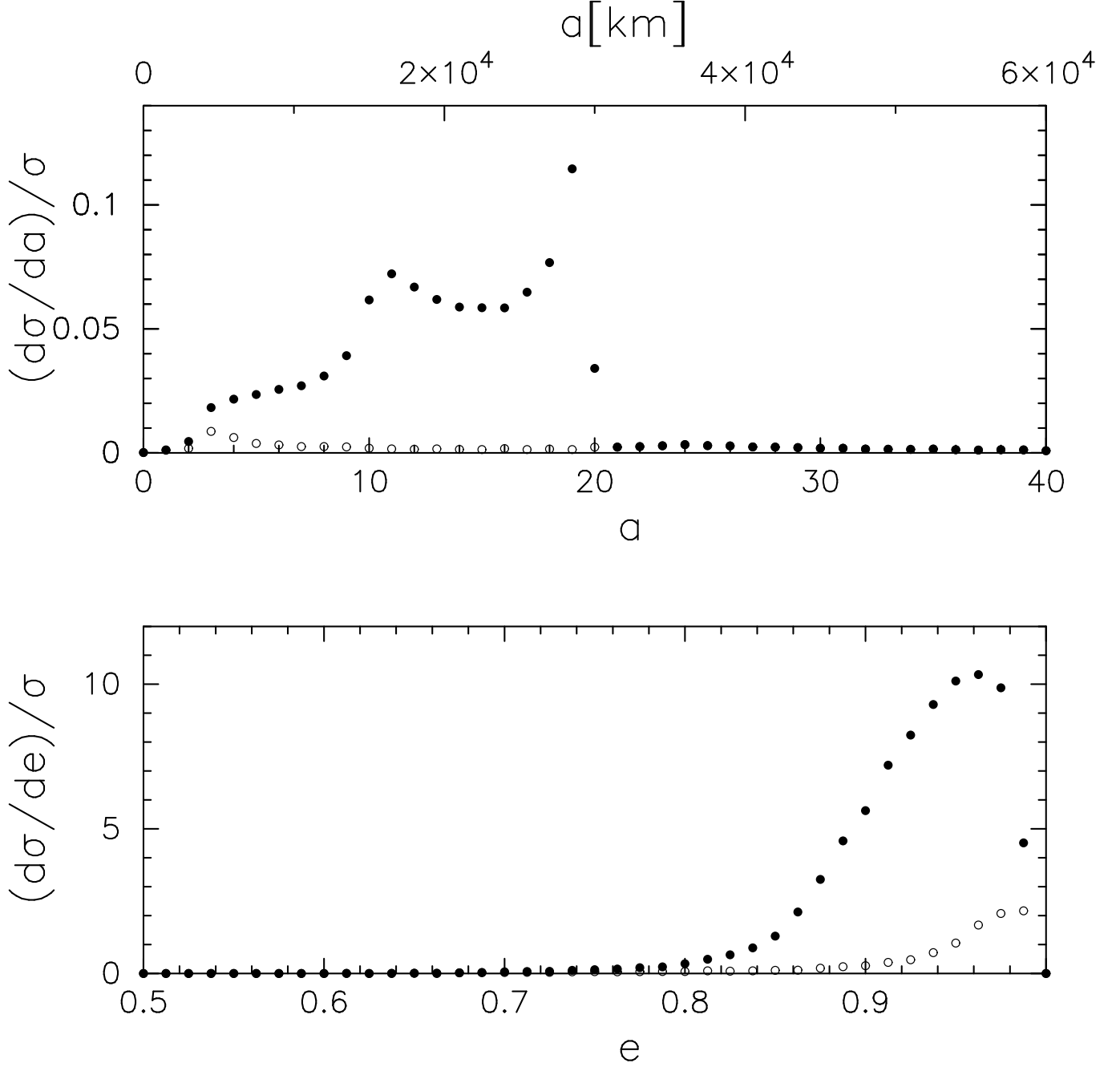


Figure 3: Normalized differential cross sections for the formation of a ‘massive-massive’ binary. Normalized differential cross sections for the event-types (a), (c) and (e) in Methods are plotted with respect to the semi-major axis a (top panel), and eccentricity e (bottom panel) of the final binary. The physical units are given for reference at the top of the figure. The filled points are the total values, while the open circles are the contributions from the merger events (types (c) and (e) in Methods).

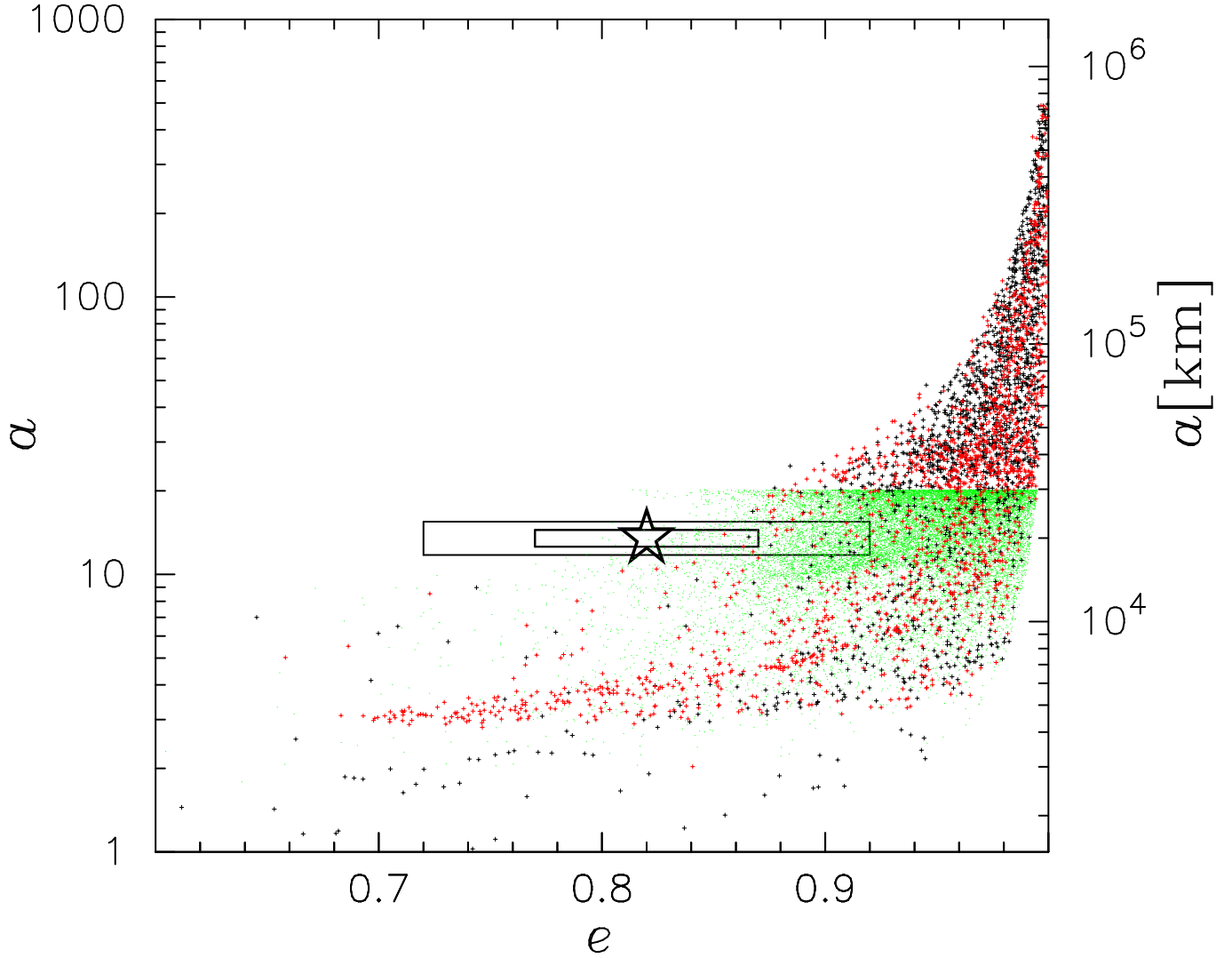


Figure 4: Distribution of orbital properties of ‘massive-massive’ binaries formed in our scattering experiments. Here a and e have the same meanings as in fig. 3. Contributions from exchange reactions, event-type (a) in Methods, are shown by green dots. They are limited by energy conservation to $a \lesssim 20$, and give rise to the horizontal rim in the middle of the figure. Contributions involving mergers, types (c, red dots) and (e, black dots), can lead to a values all the way to the Hill radius $a \approx 10^3$. The star symbol shows the observed orbit for 1998WW31. Boxes around the star indicate the observational 1- and 2- σ error bars.